Superconducting and magnetic properties of $Ru_{1-y}M_ySr_2Eu_{2-x}Ce_xCu_2O_{10+\delta}$ (M=Nb,Sn)

S. K. Goh,[1,2,*] G. V. M. Williams,[1] E. K. Hemery,[1,2] and H. K. Lee[3]
[1]*The MacDiarmid Institute for Advanced Materials and Nanotechnology, Industrial Research, P. O. Box 31310, Lower Hutt, New Zealand*
[2]*School of Chemical and Physical Sciences, Victoria University, Private Bag, Wellington, New Zealand*
[3]*Department of Physics, Kangwon National University Chunchon 200-701, Korea and Korea Basic Science Institute, Chunchon Center, Chunchon 200-701, Korea*
(Received 27 January 2006; revised manuscript received 4 May 2006; published 16 October 2006)

We have investigated the effects of isoelectronic Nb^{5+} and hole-doping Sn^{4+} substitutions for Ru^{5+} on the magnetic and electronic properties of $RuSr_2Eu_{2-x}Ce_xCu_2O_{10+\delta}$ that displays superconductivity and magnetic order. We find a rapid increase in the Meissner state onset temperature when the magnetic order is completely destroyed by Sn substitution, which we show is consistent with the spontaneous vortex phase model. The temperature characterizing the ferromagnetic component, T_M^*, and the saturation magnetization, M_s, decreases more rapidly for hole-doping by Sn than for nearly isoelectronic doping by Nb. We propose a ferrimagnetic picture to explain the magnetization data.

DOI: 10.1103/PhysRevB.74.134506 PACS number(s): 74.72.−h, 74.62.Dh, 74.25.Ha, 74.25.Fy

INTRODUCTION

The ruthenocuprates, $RuSr_2R_{2-x}Ce_xCu_2O_{10+\delta}$ and $RuSr_2RCu_2O_8$ (R=rare earth), are interesting CuO_2 and RuO_2 layered compounds that display superconductivity and magnetic order.[1–11] Despite extensive studies, the nature of magnetic order in these compounds is still an issue of great debate. $RuSr_2RCu_2O_8$ was initially believed to be ferromagnetic. However, recent neutron-diffraction data revealed that $RuSr_2RCu_2O_8$ is antiferromagnetically ordered with a small ferromagnetic component.[8,10] A spin-flop transition to a ferromagnetic state occurs as the magnetic field is increased.[9]

Unfortunately there are no neutron-diffraction data available for $RuSr_2R_{2-x}Ce_xCu_2O_{10+\delta}$ and hence it is not possible to uniquely determine the magnetic structure. Synchrotron x-ray measurements show significant rotation and tilting of the RuO_6 octahedra[12,13] that form coherent domains at low temperature for x=1 as evidenced by zone folded Raman peaks.[14] Magnetization measurements reveal a large ferromagnetic component at low temperatures that can be characterized by T_M^*, which is the temperature where the maximum negative gradient occurs. This T_M^* is ~115 K for x=1.0 and decreases to ~55 K for x=0.4.[11] It has been suggested from magnetization measurements that $RuSr_2R_{2-x}Ce_xCu_2O_{10+\delta}$ antiferromagnetically orders at temperature of up to ~190 K,[3] and Dzyaloshinsky-Moriya antisymmetric exchange coupling induces spin-canting that results in a weak ferromagnetic component below~190 K.[3] The large ferromagnetic component that occurs at lower temperatures is believed to arise from additional Ru-Ru superexchange. Unlike $RuSr_2RCu_2O_8$, the saturation field of $RuSr_2R_{2-x}Ce_xCu_2O_{10+\delta}$ (~0.2 T) is small and there is no evidence of a spin-flop transition. The large saturation magnetization at low temperatures (~1 μ_B per Ru) appears to be too large to be attributed to spin-canting and antiferromagnetism, hence it is possible that the low-temperature magnetic order is ferrimagnetic or ferromagnetic.

A number of studies have provided evidence for the coexistence of magnetic order and superconductivity.[6,15] This coexistence has been explained by a spontaneous vortex phase (SVP) model.[4,7] In the SVP model, the transition to the Meissner state occurs at the temperature $T_{\text{Meissner}} \leq T_c$, where T_c is the superconducting transition temperature. A SVP can exist for $T_{\text{Meissner}} < T < T_c$ if the superconducting sample is also magnetically ordered with a ferromagnetic component and the internal field is greater than the superconducting lower critical field. For $T \leq T_{\text{Meissner}}$, the superconducting lower critical field is assumed to be greater than the internal field from the ferromagnetic component, hence full diamagnetic shielding occurs at low temperatures. When the magnetic order is suppressed, it is expected that $T_{\text{Meissner}}=T_c$. Magnetization measurements on $Ru_{1-y}Sn_ySr_2RCu_2O_8$ support the SVP model, where it was found that $T_c - T_{\text{Meissner}}$ decreases as the concentration of Sn increases and hence the magnetic ordering temperature decreases.[16]

To better understand the superconducting and magnetic states, we performed magnetization and transport measurements on $RuSr_2R_{2-x}Ce_xCu_2O_{10+\delta}$, where Sn^{4+} and Nb^{5+} were substituted for Ru, and we report the results in this paper. These two substituents were chosen because the Ru valence is believed to be near 5+.[17,18] Hence, Nb^{5+} is expected to be an isoelectronic substitution while Sn^{4+} should also lead to hole-doping. We show below that Sn^{4+} substitution in the superconducting x=0.8 samples is consistent with the SVP model and Sn^{4+} and Nb^{5+} substitutions in the nonsuperconducting x=1.0 compound both lead to a decrease in T_M^*. Furthermore, the magnetization data can be interpreted in terms of ferrimagnetic order.

EXPERIMENTAL DETAILS

Polycrystalline $Ru_{1-y}Sn_ySr_2Eu_{2-x}Ce_xCu_2O_{10+\delta}$ and $Ru_{1-y}Nb_ySr_2Eu_{2-x}Ce_xCu_2O_{10+\delta}$ samples for this study were made using a method described elsewhere.[11,16] The samples were analyzed using x-ray diffraction with a Co $K\alpha$ x-ray tube. There was no evidence of impurity phases in the x-ray-diffraction data. Electrical resistivity measurements were made using the standard four-terminal technique. Room-

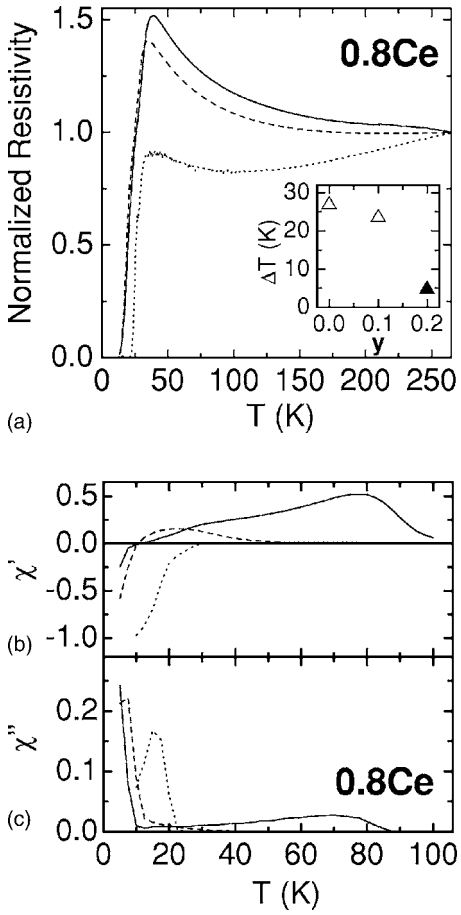

FIG. 1. (a) Plot of the normalized resistivity against temperature for $Ru_{1-y}Sn_ySr_2Eu_{1.2}Ce_{0.8}Cu_2O_{10+\delta}$ with $y=0$ (solid), $y=0.1$ (dashed), and $y=0.2$ (dotted). Inset: Plot of $\Delta T=T_c-T_{\text{Meissner}}$ vs Sn fraction y. The filled triangle in the inset is for the compound with the ferromagnetic component suppressed. (b) Plot of the real part of the ac susceptibility against temperature and (c) plot of the imaginary part of the ac susceptibility for the same samples.

temperature thermoelectric power measurements were made using the standard differential temperature method. The ac (ac field$=5\times10^{-6}$ T and frequency$=333$ Hz) and dc magnetization measurements were made using a superconducting quantum interference device (SQUID) magnetometer for temperatures up to 400 K.

RESULTS AND ANALYSIS

We first discuss the results from measurements on the superconducting $Ru_{1-y}Sn_ySr_2Eu_{1.2}Ce_{0.8}Cu_2O_{10+\delta}$ samples ($x=0.8$). This level of Ce doping is on the boundary of the superconducting phase diagram where superconductivity is observed for $0.2\leq x\leq 0.8$.[11] The normalized resistivity data are plotted in Fig. 1(a) for $y=0$ (solid line), 0.1 (dashed line), and 0.2 (dotted line). As in previous studies,[19] we take T_c, the superconducting critical temperature, as the temperature where the resistivity of the sample starts to decrease. It is apparent that the addition of Sn does not change T_c significantly. This suggests that the holes doped by Sn^{4+} substitution do not appear on the CuO_2 plane. The extra holes induced by Sn^{4+} substitution could be localized in the RuO_2 plane or they could be compensated by a decreasing oxygen content.

The doping state can be estimated from the room-temperature thermoelectric power, $S(290\text{ K})$, versus hole concentration correlation that has been reported for a wide range of high-temperature superconducting cuprates (HTSCs).[20] We find that $S(290\text{ K})$ is 20.6 μV/K for $y=0$, 28.6 μV/K for $y=0.1$, and 23.8 μV/K for $y=0.2$. Using the correlation found in other HTSCs, we estimate that the number of doped holes per Cu, p, falls in the range of $0.093<p<0.101$ for these samples. For such a small change in p, the change in T_c will not be significant,[21] and this is consistent with the results we obtained. Therefore, the addition of Sn into the RuO_2 layers does not affect T_c.

Information about T_{Meissner} can be obtained from the real (χ') and the imaginary (χ'') parts of the ac magnetization plotted in Figs. 1(b) and 1(c) for $Ru_{1-y}Sn_ySr_2Eu_{1.2}Ce_{0.8}Cu_2O_{10+\delta}$. It is clear that the ferromagnetic component of the magnetic order is visible for $Ru_{1-y}Sn_ySr_2Eu_{1.2}Ce_{0.8}Cu_2O_{10+\delta}$ with $y=0$ and 0.1 (solid and dashed lines, respectively), and that this ferromagnetic component disappears for $y=0.2$ (dotted lines). Thus, the substitution of Sn for Ru suppresses T_M^*. To characterize the disappearance of the ferromagnetic component, we calculate the temperature at which $d\chi'/dT$ has a maximum negative value as 87.0, 30.0, and 0 K for $y=0$, 0.1, and 0.2, respectively. The suppression rate for $Ru_{1-y}Sn_ySr_2Eu_{1.2}Ce_{0.8}Cu_2O_{10+\delta}$ is 5.7 K/% Sn, which corresponds to an initial decrease rate of $\partial[T_M^*(y)/T_M^*(0)]/\partial y=6.6$.

Similar to previous studies,[3,17] we take T_{Meissner} as the temperature at which $\chi'=0$. It is apparent that T_{Meissner} changes when the Sn fraction is changed, and T_{Meissner} approaches the value of T_c when the ferromagnetic component disappears at $y=0.2$. This is clearly illustrated in the inset of Fig. 1(a), where we plot $\Delta T=T_c-T_{\text{Meissner}}$ versus the Sn fraction. Thus, when the magnetic order is suppressed, ΔT is much smaller. This provides direct support for the SVP model that was proposed to explain the coexistence of superconductivity and magnetic order.

We now discuss the results from measurements on the nonsuperconducting $Ru_{1-y}(Sn,Nb)_ySr_2EuCeCu_2O_{10+\delta}$ samples, which allow us to focus on the magnetic properties. The resistivity data are plotted in Fig. 2(a). The first observation is that $Ru_{1-y}(Sn,Nb)_ySr_2EuCeCu_2O_{10+\delta}$ does not show evidence of superconductivity. There are two temperature regions over which the resistivity of $Ru_{1-y}(Sn,Nb)_ySr_2EuCeCu_2O_{10+\delta}$ exhibits different functional temperature dependence. For temperatures above $\sim$80 K, there is a small decrease in the resistivity with increasing temperature except for the pure sample ($y=0$), where the temperature dependence is similar to that observed in some underdoped HTSC. For temperatures below $\sim$80 K, there is a more rapid change in the resistivity. These features can be easily seen from the inset of Fig. 2(a), where we plot the temperature dependence of the resistivity for $Ru_{1-y}(Sn,Nb)_ySr_2EuCeCu_2O_{10+\delta}$ on a log-log scale. The resistivity data below $\sim$80 K can be fitted to a power-law temperature dependence where the exponent ranges from -0.8 to -1.1 irrespective of the dopant.

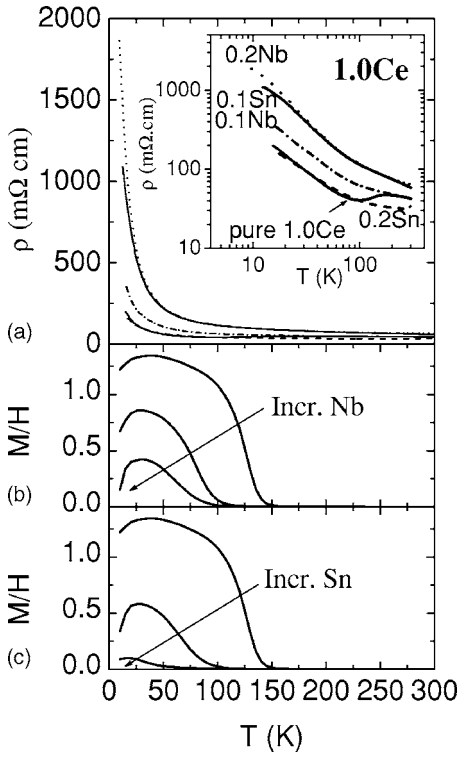

FIG. 2. (a) Plot of the resistivity against temperature for $Ru_{1-y}(Nb,Sn)_ySr_2EuCeCu_2O_{10+\delta}$ with $y=0$ (lower solid), $y=0.1$ for Sn (upper solid), $y=0.1$ for Nb (dash-dot), $y=0.2$ for Sn (dashed), and $y=0.2$ for Nb (dotted). The same datasets are re-plotted on the log-log scale in the inset. (b,c) M/H against temperature of $Ru_{1-y}(Nb,Sn)_ySr_2EuCeCu_2O_{10+\delta}$. The arrows indicate the increasing substituent fraction.

The $S(290\ \mathrm{K})$ values are also consistent with very underdoped CuO_2 planes with a hole concentration close to that where superconductivity occurs in the HTSCs. We find that $S(290\ \mathrm{K})$ is 62.6, 71.6, 100.1, 86.3, and 68.0 μV/K for $Ru_{1-y}(Sn,Nb)_ySr_2EuCeCu_2O_{10+\delta}$ with $y=0$, 0.1, and 0.2 for Nb and $y=0.1$ and 0.2 for Sn, respectively. From the correlation between p and $S(290\ \mathrm{K})$ found in a number of the HTSCs,[20] we deduce that all samples are underdoped ($p<0.16$) and p ranges from $\sim$0.04 to $\sim$0.06. These values are near the border ($p=0.05$) where superconductivity is observed ($p>0.05$). The samples with the higher $S(290\ \mathrm{K})$ (lowest p) also have the higher resistivity. For example, the resistivity of $Ru_{0.8}Sn_{0.2}Sr_2EuCeCu_2O_{10+\delta}$ is lower than that of $Ru_{0.9}Sn_{0.1}Sr_2EuCeCu_2O_{10+\delta}$ because the former has a lower $S(290\ \mathrm{K})$ and hence a higher p than the latter. The resistivity of the pure $RuSr_2EuCeCu_2O_{10+\delta}$, on the other hand, is comparable to that of $Ru_{0.8}Sn_{0.2}Sr_2EuCeCu_2O_{10+\delta}$ because of the comparable $S(290\ \mathrm{K})$ and hence comparable p. This is expected in a model where the charge transport is dominated by the CuO_2 planes and by noting that in the HTSCs the resistivity decreases with increasing p over the deduced hole concentration range. Thus, it is not possible to determine if the RuO_2 layers are conducting. A similar situation exists in $RuSr_2RCu_2O_8$ where the charge transport is dominated by the CuO_2 planes. However, from anomalous Hall effect measurements it was possible to deduce an itinerant metallic state in the RuO_2 planes.[22]

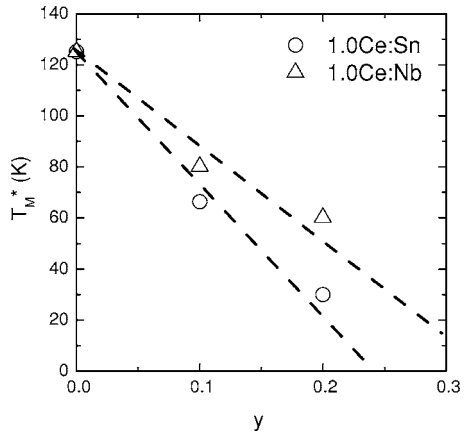

FIG. 3. Plot of T_M^* against the Sn (open circles) and Nb (open triangles) concentration y. The dotted lines are a guide to the eye.

The effect of substituents on the magnetization data can be seen in Figs. 2(b) and 2(c) where the zero-field-cooled M/H data are plotted for $Ru_{1-y}Nb_ySr_2EuCeCu_2O_{10+\delta}$ [Fig. 2(b)] and $Ru_{1-y}Sn_ySr_2EuCeCu_2O_{10+\delta}$ [Fig. 2(c)] measured at 25 mT. Following the method described in the earlier section, we find that T_M^* for Nb-substituted samples decreases from 125 K for $y=0$ to 80 K for $y=0.1$ and to 60 K for $y=0.2$. For the Sn-substituted samples, T_M^* is 125, 66, and 30 K for $y=0$, 0.1, and 0.2, respectively. Thus, Nb and Sn both suppress T_M^* and Sn substitution leads to a greater suppression rate. This is clearer in Fig. 3, where T_M^* is plotted against the substituent concentration y. The rates of suppression, estimated from the slope of the dashed lines, are 3.7 K/% Nb and 5.2 K/% Sn. These correspond to $\partial[T_M^*(y)/T_M^*(0)]/\partial y$ of 3.0 and 4.2, respectively. The rate of suppression of T_M^* by Sn and Nb is comparable to that found in antiferromagnetically ordered $Ru_{1-y}Sn_ySr_2GdCu_2O_8$, where $\partial[T_N(y)/T_N(0)]/\partial y=3.8$ and T_N is the Neel temperature.[16] The rates of suppression are also similar to those found in the quasi-2D antiferromagnetic compounds $La_2Cu_{1-x}Mg_xO_4$ ($\partial[T_N(y)/T_N(0)]/\partial y\sim 3.0$ (Ref. 23)) and $La_2Cu_{1-y}(Mg,Zn)_yO_4$ ($\partial[T_N(y)/T_N(0)]/\partial y\sim 3.7$ (Ref. 24)). In the case of $La_2Cu_{1-y}(Mg,Zn)_yO_4$, the suppression of T_N was consistent with a randomly site diluted nearest-neighbor square lattice Heisenberg antiferromagnet with a site percolation threshold of $y\sim 0.41$.[24] Although the nature of the magnetic order in $RuSr_2EuCeCu_2O_{10+\delta}$ is not clear, the comparison with $La_2Cu_{1-y}(Mg,Zn)_yO_4$ suggests that the decrease in T_M^* may arise from random site dilution.

The low-temperature magnetic state was probed by magnetization measurements as a function of applied field. The resultant data are plotted in Fig. 4 for measurements on $Ru_{1-y}(Sn,Nb)_ySr_2EuCeCu_2O_{10+\delta}$ at 5 K and after subtracting the Van Vleck paramagnetic contribution from $Eu^{3+}(^7F_0)$. The Van Vleck contribution was calculated in a manner similar to that done in a previous high-temperature susceptibility study on $RuSr_2EuCu_2O_8$,[25] and we used a spin-orbit coupling constant of 303 cm^{-1} as measured in Eu_2CuO_4.[26] The magnetic moment per formula unit (f.u.) is plotted in units of the Bohr magneton, μ_B, and we find that it increases rapidly at relatively low applied magnetic field where the saturation

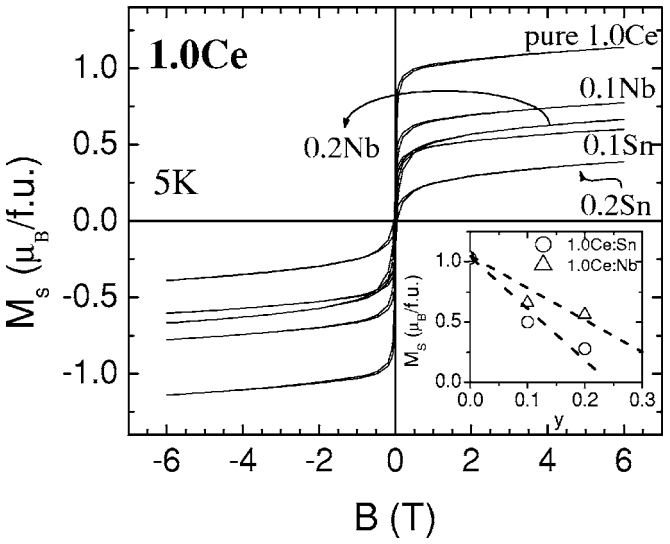

FIG. 4. Plot of the magnetic moment per formula unit vs the applied magnetic field for $Ru_{1-y}(Nb,Sn)_ySr_2EuCeCu_2O_{10+\delta}$. The Nb and Sn concentrations are shown in the figure. Inset: Plot of M_s vs the Sn (open circles) or Nb (open triangles) concentration y.

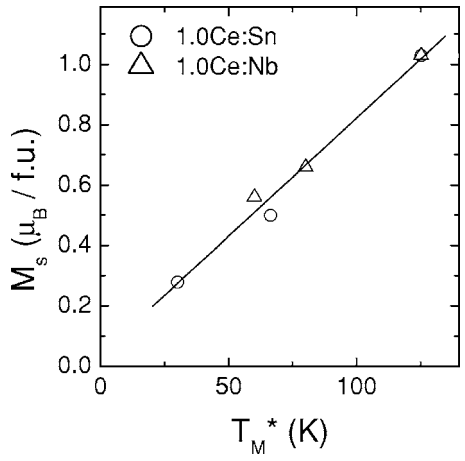

FIG. 5. Plot of the saturation moment M_s vs T_M^* for $Ru_{1-y}Sn_ySr_2EuCeCu_2O_{10+\delta}$ (open circles) and $Ru_{1-y}Nb_ySr_2EuCeCu_2O_{10+\delta}$ (open up triangles). The solid line is the linear best fit to the data.

field is ~0.2 T. Similar to previous studies, we find that the remanent magnetization ($0.42\mu_B$/f.u.) and 6 T magnetization ($1.14\mu_B$/f.u.) from the pure compound are large and there is no evidence for a spin-flop transition. These features are the typical characteristics of ferromagnetically or ferrimagnetically ordered materials.

It is apparent in Fig. 4 that the introduction of substituents into the ruthenium layers decreases the high-field moment per Ru site. The high-field moment per Ru site at 6 T is $1.14\mu_B$/f.u. for $RuSr_2EuCeCu_2O_{10+\delta}$. If $RuSr_2EuCeCu_2O_{10+\delta}$ is ferromagnetic and Ru^{5+} is in the high-spin state ($S=3/2$), then the saturation moment is expected to be $3\mu_B$, as calculated from $M_s=gS$, where g is the Lande g factor, which is taken as 2.00, and S is the total spin. If Ru^{5+} is in the low-spin state ($S=1/2$), then the saturation moment is expected to be $1\mu_B$. The moment obtained at 6 T is close to the saturation moment of Ru^{5+} in low-spin state, which suggests ferromagnetic order and a low-spin electronic configuration. However, we show later that this possibility is inconsistent with the high-temperature effective moment in the Curie-Weiss regime, and ferrimagnetic order is possible.

The high-field magnetization is linear in H and we use a linear extrapolation of the high-field magnetization to estimate the saturation magnetization, M_s. For the pure compound $M_s=1.07\mu_B$/f.u., which is slightly smaller than the value at 6 T. M_s is plotted against the Sn or Nb fraction in the right lower inset to Fig. 4. We find that the rate of suppression is more rapid for Sn substituted samples. The rate of suppression for Sn substitution appears to be too large to be accounted for within a randomly site diluted nearest-neighbor 2D Heisenberg model.[24] However, the Monte Carlo simulations were done for $S=1/2$ and we show later that the magnetic order may be ferrimagnetic with a mixture of $S=1/2$ and 3/2. This may affect the rate at which M_s is suppressed. A complete analysis can only be done when neutron-diffraction data are available and when Monte Carlo simulations are made that take into account the possible ferrimagnetic order.

While T_M^* and M_s are more rapidly suppressed by Sn substitution, we find a linear correlation between M_s and T_M^* for Sn and Nb that can be seen in Fig. 5. The linear correlation is evident by the solid line, which is a linear fit to the data. Thus, while Sn suppresses T_M^* faster than Nb, we find a common $M_s(T_M^*)$ for the Sn and Nb concentrations studied. A linear correlation is found in $RuSr_2EuCu_2O_8$, where Sn is partially substituted for Ru and where M_s is measured at 6 T.[16]

Additional information about the magnetic state can be obtained from the effective moment in the Curie-Weiss temperature regime where M/H is independent of $H(>175$ K). Typical data are plotted in Fig. 6 for the pure compound (open circles). The data can be understood by noting that M/H can be written as

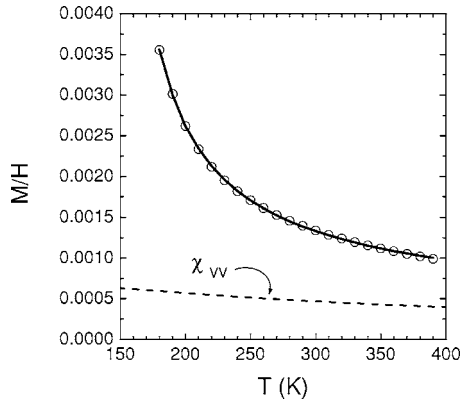

FIG. 6. Plot of raw M/H data against temperature up to 400 K for $RuSr_2EuCeCu_2O_{10+\delta}$ (open circles). The solid line is the fit to the data using Eq. (1) and the dashed line is the Van Vleck paramagnetic contribution of Eu^{3+} as described in the text.

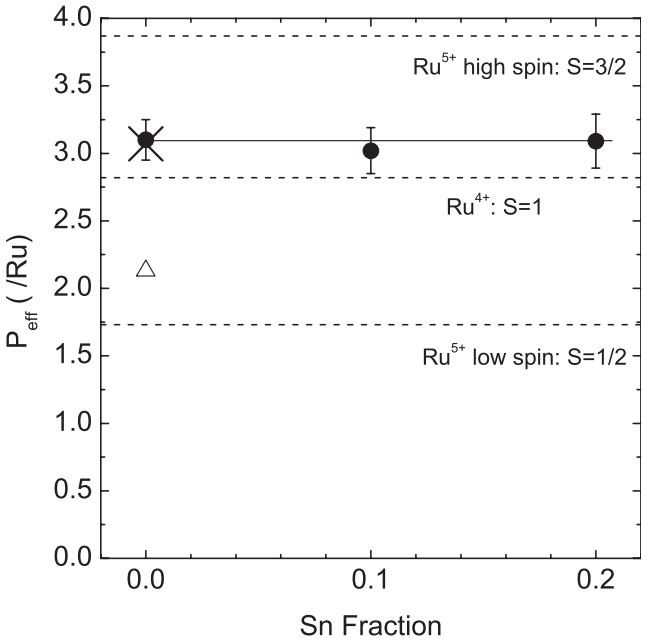

FIG. 7. Plot of the effective Bohr magneton number P_{eff} for $Ru_{1-y}Sn_ySr_2EuCeCu_2O_{10+\delta}$ with different Sn fractions (filled circles). The cross is the data of Butera *et al.* (Ref. 28) and the open triangle is the data of Felner *et al.* (Ref. 29), both for $RuSr_2EuCeCu_2O_{10+\delta}$ (i.e., $y=0$). The theoretical values of P_{eff} with different S are shown as the dashed lines in the figure and the solid line assumes a fixed Ru^{5+} low-spin (45%) and high-spin (55%) configuration.

$$\frac{M}{H} = \frac{C}{T-\vartheta} + \chi_{VV}(T) + \chi_0. \tag{1}$$

The first term in Eq. (1) is the Curie-Weiss term from the Ru moments, where ϑ is the Curie-Weiss temperature and the Curie constant is

$$C = \frac{N}{V}\frac{\mu_0 P_{\text{eff}}^2 \mu_B^2 (1-y)}{3k_B}, \tag{2}$$

where μ_0 is the vacuum permeability, P_{eff} is the effective moment per Ru in units of μ_B, k_B is the Boltzmann constant, $(1-y)$ is the number of Ru atoms per f.u., and N/V is the number of Ru atoms per unit volume in the pure compound. The second term in Eq. (1) is the Van Vleck susceptibility from $Eu^{3+}(^7F_0)$. The Van Vleck susceptibility from Eu^{3+} is plotted in Fig. 6 (dashed curve). The third term accounts for the susceptibility from the CuO_2 planes and any temperature-independent susceptibility from the RuO_2 planes. The spin susceptibility from the CuO_2 planes in the HTSCs is small ($<0.4\times10^{-4}$, Ref. 27) and hence we approximate it as a constant for temperatures above 175 K.

It can be seen in Fig. 6 that Eq. (1) provides a good fit to the data (solid curve). After fitting the data for the Sn-substituted samples, we find that ϑ is 138, 127, and 95 K for $y=0$, 0.1, and 0.2, respectively. The measured P_{eff} are plotted in Fig. 7 for the Sn-substituted (filled circles) samples. Thus, we find that the Curie-Weiss temperature decreases while P_{eff} remains nearly the same for increasing Sn concentration. The value we obtained for the pure 1.0Ce sample is 3.10 ± 0.15/Ru. This value is close to that obtained by Butera *et al.* (cross, 3.07/Ru).[28] However, it is significantly greater than the value obtained by Felner *et al.* (open triangle, 2.13/Ru).[29] None of these P_{eff} values corresponds to any of the theoretical values calculated from various high- and low-spin states of Ru^{4+} and Ru^{5+} (dashed lines).

The value of $P_{\text{eff}}=3.10\pm0.15$/Ru for the pure 1.0Ce suggests the existence of a mixed valence. This has already been observed in $RuSr_2RCu_2O_8$, where $\sim40-50$ % Ru^{4+} and $\sim60-50$ % Ru^{5+} has been deduced from magnetization,[30] nuclear magnetic resonance,[31,32] and x-ray-absorption near-edge spectroscopy (XANES) (Ref. 33) data. However, a mixed Ru^{4+} and Ru^{5+} valence is unlikely in $RuSr_2EuCeCu_2O_{10+\delta}$ because the predicated valence is inconsistent with the Ru valence near 5+ that was measured by XANES.[18] The Ru valence required to account for the measured effective moment can be estimated from

$$P_{\text{eff}}^{\text{tot}} = \sqrt{f_{4+}(P_{\text{eff}}^{4+})^2 + f_{5+}(P_{\text{eff}}^{5+})^2}, \tag{3}$$

where f_{4+}, f_{5+} are the fractions of Ru^{4+} and Ru^{5+}, respectively, and P_{eff}^{4+} and P_{eff}^{5+} are the effective moments for Ru^{4+} and Ru^{5+}, which can be obtained from $P_{\text{eff}}^{v}=g\sqrt{S_v(S_v+1)}$. Taking $S_{4+}=1$, $S_{5+}=3/2$, and $P_{\text{eff}}^{\text{tot}}=3.1$/Ru, it can be calculated that 77% of Ru^{4+} and 23% of Ru^{5+} are required, which makes the effective valence of +4.23. However, the valence of +4.23 is inconsistent with the $\sim+5$ valence obtained using other experimental methods.[17,18]

It has been suggested by Felner *et al.*[29] that Ru^{5+} is in a low-spin configuration with $S_{\text{LS}}=1/2$, however it can be seen in Fig. 7 that 100% of Ru^{5+} in the low-spin configuration cannot account for the measured effective moment. Therefore, we propose a mixture of Ru^{5+} in the low-spin configuration with $S_{\text{LS}}=1/2$ and the high-spin configuration with $S_{\text{HS}}=3/2$. According to Hund's rule, the stable electronic configuration of Ru^{5+} for a perfect octahedral crystal field would have three valence electrons occupying the lower three t_{2g} orbitals, which leads to the high-spin state with $S_{\text{HS}}=3/2$. However, octahedral distortion can lead to a splitting of the lower t_{2g} orbitals into one higher-energy and two lower-energy orbitals. This is observed in some other transition-metal oxides, including the HTSCs.[34] Thus, the low-spin configuration could arise from regions with distorted octahedra where only the two lower t_{2g} levels are occupied and leading to the low-spin $S_{\text{LS}}=1/2$ suggestion of Felner *et al.*[29] By repeating the calculation above, we obtain $f_{\text{HS}}\sim55\%$ and $f_{\text{LS}}\sim45\%$ for the fractions of Ru^{5+} in its high-spin state and low-spin state, respectively, for the pure compound.

To maintain overall charge neutrality, the partial substitution of Sn^{4+} for Ru^{5+} needs to be compensated for by an increase in the Ru valence, a decrease in the Cu valence, or a reduction in the oxygen content. If the main change is a reduction in the oxygen content and a small change in the Cu valence, then it is possible that the Ru valence remains at 5+ at least for up to 0.2 Sn. In this scenario, the fraction of Ru atoms in the low-spin and high-spin configurations might not be expected to change with increasing Sn concentration.

This is consistent with the data, as can be seen in Fig. 7 (solid line).

A mixture of Ru^{5+} high-spin and low-spin configurations as well as ferrimagnetic order can also account for the saturation magnetization at low temperatures. Taking the f_{HS} and f_{LS} values estimated from the Curie-Weiss temperature regime and assuming that the low-spin and high-spin moments are antiparallel results in a saturation moment of $\sim 1.2\mu_B$/f.u., which is close to the measured value of $1.07\mu_B$/f.u. When the experimental uncertainty in the measured P_{eff} is accounted for, we obtain an expected saturation moment of $1.16\pm 0.24\mu_B$/f.u.

CONCLUSION

In conclusion, we have probed the superconducting and magnetic order in $RuSr_2Eu_{2-x}Ce_xCu_2O_{10+\delta}$ by the partial substitution of Ru^{5+} by Nb^{5+} and Sn^{4+}, which are isoelectronic and hole dopants, respectively. For superconducting and magnetically ordered $RuSr_2Eu_{1.2}Ce_{0.8}Cu_2O_{10+\delta}$, we found a rapid suppression of the ferromagnetic component when Sn is partially substituted for Ru. In addition, we observed a decrease in $T_c - T_{\text{Meissner}}$ when the ferromagnetic component disappeared, which provides support for the spontaneous vortex phase model that is believed to account for the coexistence of magnetic and superconducting order.

The magnetic order was probed in nonsuperconducting $RuSr_2EuCeCu_2O_{10+\delta}$. We found that T_M^* and M_s are suppressed by Sn^{4+} and Nb^{5+} but the suppression is more rapid for Sn^{4+}. Even though T_M^* and M_s are suppressed at different rates by Sn^{4+} and Nb^{5+}, we find that M_s is a linear function of T_M^* and the Sn^{4+} and Nb^{5+} data fall on a common curve. We have shown that the high-temperature effective moment can be accounted for by a mixture of high-spin and low-spin Ru^{5+} electronic configurations and this model is also consistent with the nearly Sn concentration independent change in the effective moment. It is also possible within this model to account for the low-temperature saturation moment in terms of ferrimagnetic order.

ACKNOWLEDGMENTS

We acknowledge funding support by the New Zealand Marsden Fund, the Alexander von Humboldt Foundation (GVMW), Industrial Research Limited (SKG), and the MacDiarmid Institute for Advanced Materials and Nanotechnology (EKH). We also thank Jeff Tallon and Neil Ashcroft for useful comments.

*Present address: Quantum Matter Group, Cavendish Laboratory, University of Cambridge, J J Thomson Avenue, Cambridge CB3 0HE, United Kingdom.

[1] L. Bauernfeind, W. Widder, and H. F. Braun, Physica C **254**, 151 (1995).
[2] L. Bauernfeind, W. Widder, and H. F. Braun, J. Low Temp. Phys. **105**, 1605 (1996).
[3] I. Felner, U. Asaf, and O. Millo, Phys. Rev. B **55**, R3374 (1997).
[4] E. B. Sonin and I. Felner, Phys. Rev. B **57**, R14000 (1998).
[5] I. Felner, U. Asaf, S. Reich, and Y. Tsabba, Physica C **311**, 163 (1999).
[6] C. Bernhard, J. L. Tallon, Ch. Neidermayer, Th. Blasius, A. Golnik, E. Brücher, R. K. Kremer, D. R. Noakes, C. E. Stronach, and E. J. Ansaldo, Phys. Rev. B **59**, 14099 (1999).
[7] C. Bernhard, J. L. Tallon, E. Bruecher, and R. K. Kremer, Phys. Rev. B **61**, R14960 (2000).
[8] J. W. Lynn, B. Keimer, C. Ulrich, C. Bernhard, and J. L. Tallon, Phys. Rev. B **61**, R14964 (2000).
[9] G. V. M. Williams and S. Krämer, Phys. Rev. B **62**, 4132 (2000).
[10] J. D. Jorgensen, O. Chmaissem, H. Shaked, S. Short, P. W. Klamut, B. Dabrowski, and J. L. Tallon, Phys. Rev. B **63**, 054440 (2001).
[11] G. V. M. Williams and M. Ryan, Phys. Rev. B **64**, 094515 (2001).
[12] G. V. M. Williams, A. C. McLaughlin, J. P. Attfield, S. Krämer, and H. K. Lee (unpublished).
[13] A. C. Mclaughlin, J. P. Attfield, U. Asaf, and I. Felner, Phys. Rev. B **68**, 014503 (2003).
[14] A. Fainstein, R. G. Pregliasco, G. V. M. Williams, and H. J. Trodahl, Phys. Rev. B **65**, 184517 (2002).
[15] A. Shengelaya, R. Khasanov, D. G. Eschenko, I. Felner, U. Asaf, I. M. Savić, H. Keller, and K. A. Müller, Phys. Rev. B **69**, 024517 (2004).
[16] G. V. M. Williams, H. K. Lee, and S. Krämer, Phys. Rev. B **67**, 104514 (2003).
[17] I. Felner, U. Asaf, C. Godart, and E. Alleno, Physica B **259–261** 703 (1999).
[18] G. V. M. Williams, L. Y. Jang, and R. S. Liu, Phys. Rev. B **65**, 064508 (2002).
[19] J. L. Tallon, J. W. Loram, G. V. M. Williams, and C. Bernhard, Phys. Rev. B **61**, R6471 (2000).
[20] J. L. Tallon, C. Bernhard, H. Shaked, R. L. Hitterman, and J. D. Jorgensen, Phys. Rev. B **51**, 12911 (1995).
[21] M. R. Presland, J. L. Tallon, R. G. Buckley, R. S. Liu, and N. E. Flower, Physica C **176**, 95 (1991).
[22] M. Požek, A. Dulčić, D. Paar, A. Hamzić, M. Basletić, E. Tafra, G. V. M. Williams, and S. Krämer, Phys. Rev. B **65**, 174514 (2002).
[23] S.-W. Cheong, A. S. Cooper, L. W. Rupp, Jr., B. Batlogg, J. D. Thompson, and Z. Fisk, Phys. Rev. B **44**, 9739 (1991).
[24] O. P. Vajk, P. K. Mang, M. Greven, P. M. Gehring, and J. W. Lynn, Science **295**, 1691 (2002); O. P. Vajk, M. Greven, P. K. Mang, and J. W. Lynn, Solid State Commun. **126**, 93 (2003).
[25] A. Butera, A. Fainstein, E. Winkler, and J. Tallon, Phys. Rev. B **63**, 054442 (2001).
[26] M. Tovar, D. Rao, J. Barnett, S. B. Oseroff, J. D. Thompson, S-W. Cheong, Z. Fisk, D. C. Vier, and S. Schultz, Phys. Rev. B **39**, 2661 (1989).
[27] M. Takigawa, A. P. Reyes, P. C. Hammel, J. D. Thompson, R. H. Heffner, Z. Fisk, and K. C. Ott, Phys. Rev. B **43**, 247 (1991).
[28] A. Butera, M. V. Mansilla, A. Fainstein, and G. V. M. Williams, Physica B **320**, 316 (2002).
[29] I. Felner, U. Asaf, and E. Galstyan, Phys. Rev. B **66**, 024503 (2002).
[30] A. Butera, A. Fainstein, E. Winkler, and J. Tallon, Phys. Rev. B

63, 054442 (2001).
[31] Y. Tokunaga, H. Kotegawa, K. Ishida, Y. Kitaoka, H. Takagiwa, and J. Akimitsu, Phys. Rev. Lett. **86**, 5767 (2001).
[32] K. Kumagai, S. Takada, and Y. Furukawa, Phys. Rev. B **63**, 180509(R) (2001).
[33] R. S. Liu, L.-Y. Jang, H.-H. Hung, and J. L. Tallon, Phys. Rev. B **63**, 212507 (2001).
[34] S. E. Barrett, D. J. Durand, C. H. Pennington, C. P. Slichter, T. A. Friedmann, J. P. Rice, and D. M. Ginsberg, Phys. Rev. B **41**, 6283 (1990).